

## Chapter 2

# Conventional Machining Operations

Despite the fact that fiber-reinforced polymer components (FRP) are mostly produced near net shape, machining is often required in order to bring the component into dimensional requirements and prepare it for assembly. Machining of FRPs may take place before and/or after layup and curing. The machining before curing involves cutting the reinforcement material to the proper size to fit the contour before it is laid in/onto a mold and cured. The reinforcement material is either dry or resin impregnated fibers, fiber weaves, and fabrics. The predominantly two-dimensional contouring is most appropriately carried out by cutting techniques common to the textiles industry. These include ultrasonic cutting, reciprocating knife, shearing, and punching. Waterjet cutting and laser beam are also widely used. Cutting of prepregs and dry reinforcement is beyond the scope of this book and will not be discussed here. Our discussion is focused on the more important processes of machining of cured composites.

Machining of cured FRPs is carried out by conventional or nonconventional material removal methods. The conventional methods most frequently used are edge trimming, milling, drilling, countersinking, turning, sawing, and grinding. Among the nonconventional machining processes are abrasive waterjet and laser beam cutting. Some of these processes were originally developed either for the woodworking or for the metal working industries. However, they were conveniently transferred to machining FRPs after proper adjustments to tool geometry, cutting speeds, and feed rates are made. Nevertheless, kinematics of the machining process remains the same and most of the kinematic relationships in metal machining still hold. This chapter provides a discussion of the most important kinematics relationships for conventional machining processes that are frequently used in machining cured FRPs. Detailed analysis of these and other machining processes can be found in [1–3].

## 2.1 Requirements for Machining FRPs

Machining FRPs is different in many aspects from machining metals. FRPs are inhomogeneous materials that consist of distinctly different phases. The reinforcement fibers are strong and brittle and may have poor thermal conductivity, as in the case of aramid and glass fibers. The polymer matrix, on the other hand, is weak and somewhat ductile. Its thermal properties are poor and its tolerance for high temperatures is a limiting factor in postcure processing. The machining of most homogeneous and ductile metals is characterized by shearing and plastic deformation and the shearing action forms a continuous chip that flows on the tool face. Eventually, under fixed cutting conditions the cutting process reaches a steady state for which the cutting forces, cutting temperatures, and surface conditions could be predicted to an acceptable accuracy. The machining of FRPs, on the other hand, is characterized by uncontrolled intermittent fracture. Oscillating cutting forces are typical because of the intermittent fracture of the fibers. The machinability of FRPs is primarily determined by the physical and mechanical properties of the fiber and matrix, fiber content, and fiber orientation. While glass and carbon fibers break in a brittle manner ahead of the cutting edge, the tougher aramid fibers evade shearing and tend to bend ahead of the advancing cutting edge. Thus the surface quality of the machined edge is greatly affected by the type of fiber reinforcement and its orientation. The cutting forces are also dependent on the fibers as the matrix strength is typically inferior to that of the fibers.

The cutting temperatures are also affected by the thermal properties and orientation of the fibers. Carbon fibers are more capable of conducting heat along their direction than glass or aramid fibers and thus are responsible for dissipating heat away from the cutting zone. The polymeric matrix is not capable of withstanding high temperatures common in machining metals and precautions should be made not to expose the matrix to excessive heat for a prolonged time. During the application of coolant, moisture absorption by the matrix or fibers may jeopardize form, dimensional accuracy, and mechanical properties of the machined part. Different thermal expansion coefficients of matrix and fibers lead to thermal stresses which may result in deformation and part damage.

Machined edge quality is the deciding factor when evaluating the machinability of FRPs. The term “quality” refers to both geometric features and the extent of material damage caused by the machining process. The measurement of both of these criteria is much more difficult for FRPs than for metals because of the inhomogeneous structure of the former. At present, commonly accepted standards of measurement techniques and characteristic indices do not exist. The aviation industry, which is becoming a substantial beneficiary of composites technology, has the most stringent requirements on machining quality. Delamination is not tolerated on components that are classified as primary structural components while some repairable delamination may be tolerated on secondary components. Delamination is caused by the low interlaminar strength of the composite structure and high transverse forces resulting from cutting. High cutting forces, in turn result from the use of improper speeds and feeds, improper tool geometry and tool wear.

Tool materials in machining composites should be capable of withstanding the abrasiveness of fibers and debris resulting from machining. The tool geometry should provide a keen edge capable of neatly shearing the fibers. These two requirements are distinctively different from those expected of a cutting tool in metal machining.

## 2.2 Turning

Turning utilizes a single cutting tool to create a surface of revolution. The cylindrical workpiece is rotated around its axis while a cutting tool is fed parallel to the axis of rotation. As the cutting tool is engaged into the workpiece, a new surface of revolution is generated by removing a layer of material whose thickness is equal to the depth of the tool engagement. A typical machine tool that generates the necessary motions for carrying out this operation is an engine lathe. A typical engine lathe is shown in Fig. 2.1. CNC lathe operates on similar kinematics principles.

The machine tool provides a primary motion to the workpiece in revolutions per minute and a secondary motion to the cutting tool in millimeters per revolution. The combined motion that generates the surface is the vector addition of these two motions. For most practical applications, the feed motion is much smaller than the primary motion and the cutting speed is determined by the primary motion alone.

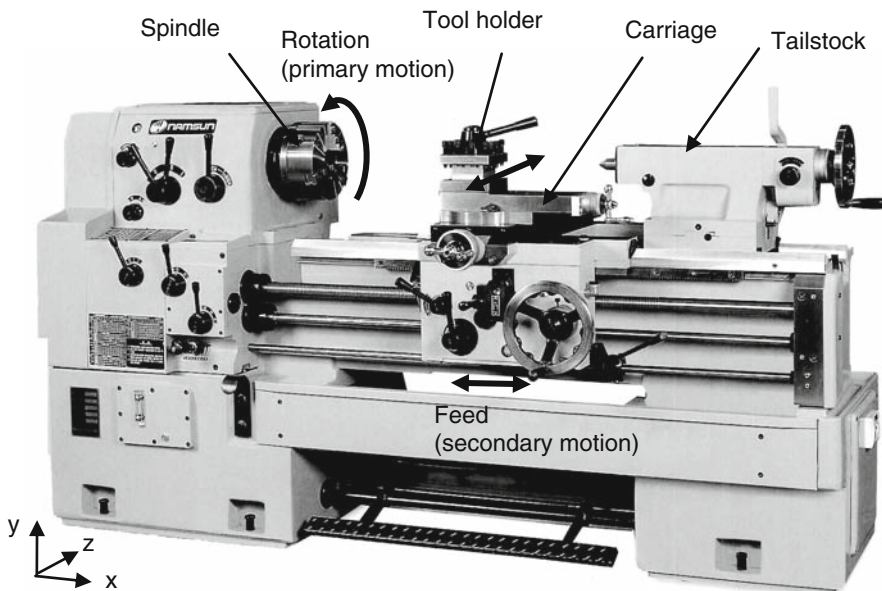


**Fig. 2.1** Principal components and movements of a typical lathe

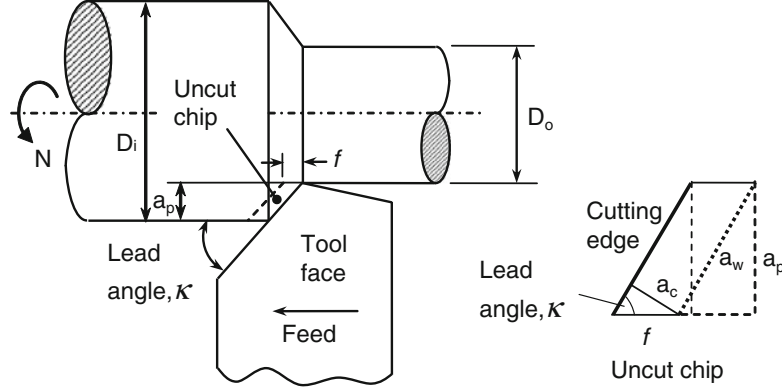


**Fig. 2.2** Cutting geometry in turning

The following relationships apply to single point tools with small corner radius or when the depth of cut is very large as compared to the corner radius. Fig. 2.2 shows the cutting geometry with a single point cutting tool.

The cutting speed is determined by the rotational speed of the spindle,  $N$ , given in rev/min, and the workpiece initial and final diameters,  $D_i$  and  $D_o$ , respectively

$$v = \pi N \frac{D_i + D_o}{2} \cong \pi N D_i. \quad (2.1)$$

The average feed motion advances the tool per revolution along a specified direction. The feed,  $f$ , is given in mm/rev and the feed speed,  $v_f$ , is related to the feed by

$$v_f = fN \quad (2.2)$$

The radial depth of cut describes the thickness of material removed from the workpiece and is given by

$$a_p = \frac{D_i - D_o}{2}. \quad (2.3)$$

This material is removed in the form of a chip (swarf) which flows upward on the tool rake face. The uncut chip thickness is measured normal to the cutting edge and is given by:

$$a_c = f \sin \kappa, \quad (2.4)$$

where  $\kappa$  is the cutting edge lead angle. The width of the uncut chip is given by

$$a_w = a_p / \sin \kappa. \quad (2.5)$$

Therefore, the uncut chip cross-sectional area is given by

$$A_c = a_c a_w = f a_p. \quad (2.6)$$

The material removal rate,  $Z_w$ , is given as the product of cutting speed and uncut chip area

$$Z_w \approx A_c v = f a_p v = \pi f a_p N D_i. \quad (2.7)$$

The time required for turning a length,  $l_w$ , in the feed direction is given by

$$t_m = \frac{l_w}{v_f} = \frac{l_w}{fN}. \quad (2.8)$$

The specific cutting power, also referred to as specific cutting pressure, is the net power required to remove a unit volume of the material in a unit time. It is related to the cutting force in the direction of cutting speed,  $F_c$ , and to the material removal rate by

$$u_s = \frac{F_c v}{Z_w} = \frac{F_c}{A_c}. \quad (2.9)$$

Then the power required to remove material is given by the product of material removal rate and specific cutting power for the workpiece material,  $u_s$

$$P_m = u_s \cdot Z_w. \quad (2.10)$$

The spindle motor power can be estimated as:

$$P_e = \frac{P_m}{\eta} + P_i, \quad (2.11)$$

where  $P_i$  is the idling power and  $\eta$  is the drive system efficiency.

## 2.3 Single Point Cutting Tools

Single point cutting tools are the primary cutting tools used in turning. These tools have a single cutting surface and a single cutting edge that is responsible for material removal. The active cutting element is shaped by three oblique surfaces that meet at the tool corner or nose. The geometry of a standard single point cutting tool is shown in Fig. 2.3. The three surfaces making the cutting element are the rake face, flank face, and heel. The inclination of these surfaces with respect to the shank defines a set of angles that are used along with the corner radius as the tool identification, or signature. During cutting the chip flows on the rake face and its flow direction is affected by the rake angles. The forces generated are also affected by the rake angles and the lead angle. The purpose of the side and end relief angles is to provide clearance between the cutting element and the workpiece surface. The side relief angle profoundly influences flank tool wear. Traditionally, single point cutting tools were ground from high-speed steel blanks. The toughness of high-speed steel allows it to be ground to a keen cutting edge, which is highly desirable when machining FRPs. A sharp cutting edge in combination with a positive rake angle allows the fibers to be neatly sheared and thus provides a good surface roughness. However, high-speed steel tools wear quite rapidly when machining FRPs because of the high abrasiveness of the fibers, and their use generally becomes impractical. Steel shanks holders tipped with brazed or indexable carbide inserts (Fig. 2.4) are more commonly used.

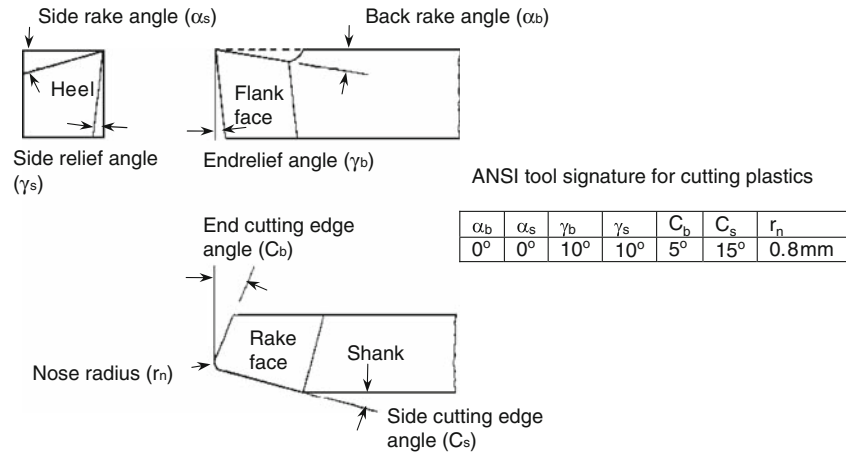


**Fig. 2.3** Standard ANSI terminology describing a single point cutting tool

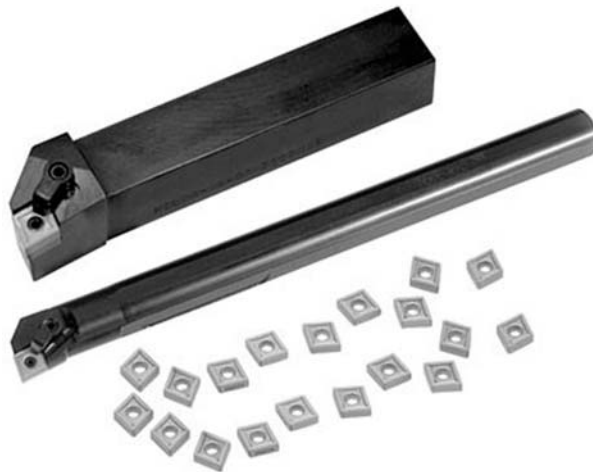


**Fig. 2.4** Typical insert tipped single point turning and boring tools

## 2.4 Milling and Trimming

In milling, material is removed from the workpiece by a rotating cutterhead that may have more than one active cutting edge. The types of milling operations that are most common in machining FRPs are peripheral milling or profiling and end milling. Figure 2.5 illustrates these milling operations. Peripheral milling uses the cutting edges on the periphery of the tool. The machined surface is parallel to the

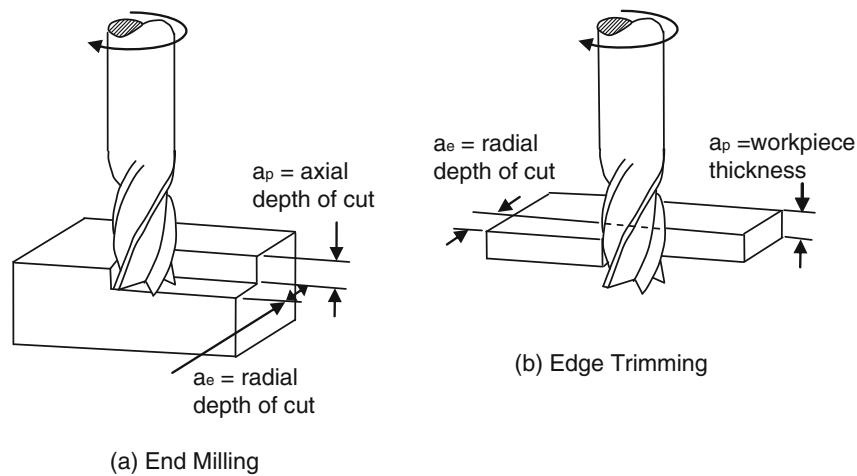


**Fig. 2.5** Types of milling operations

axis of rotation of the cutter and the engagement into the workpiece is in the radial direction of the cutter (Fig. 2.5b). Peripheral milling is more appropriately called edge trimming because the tool diameter is usually small and the axial engagement encompasses the entire thickness of the workpiece. End milling is similar to peripheral milling, except that the axial engagement may be less than the thickness of the part and a slot is obtained (Fig. 2.5a). The machine tool most commonly used is a vertical milling machine. The machine tool provides the primary motion to the spindle (to which the cutter is held) and feed motions to the machine table (to which the workpiece is held). CNC routers capable of providing higher spindle speeds and feed rates, more flexibility, and larger workspace than a typical milling machine are commonly used in high production facilities. Figure 2.6 shows the principal components and movements of typical industrial three-axis CNC router. Hand-held routers are commonly used for edge trimming of thin workpiece. The router provides the primary rotational motion to the cutter while the operator feeds the tool into the workpiece manually.

End milling and trimming operations are further classified into up (or conventional) milling and down (or climb) milling, depending on how the cutting edge approaches the workpiece. These operations are illustrated in Fig. 2.7. In up milling, the direction of cutting speed of the edge in contact with the workpiece is opposite to the direction of feed. In down milling, the direction of the cutting speed is the same as that of the feed. The resulting chip area in both cases has a “comma” shape and the length of the chip is described by a trochoid that results from the superposition of peripheral motion and feed motion. In up milling the cutting edge begins engaging the chip at the thin section of the comma shape. This results in low engagement forces and in lifting up of the workpiece. In down milling, the cutting edge engages the chip at the thick section of the comma shape. The engagement forces are high

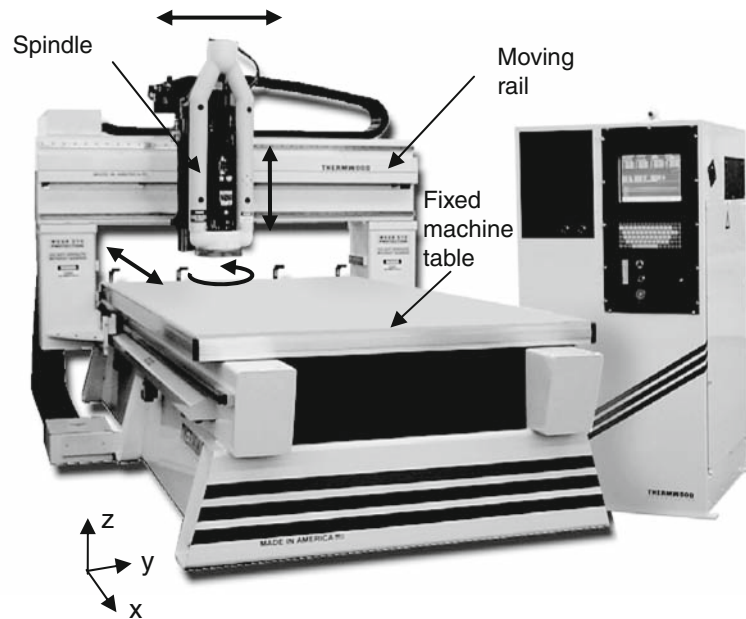


**Fig. 2.6** Principal components and movements of a three-axis gantry bridge router (courtesy of Thermwood Corporation)

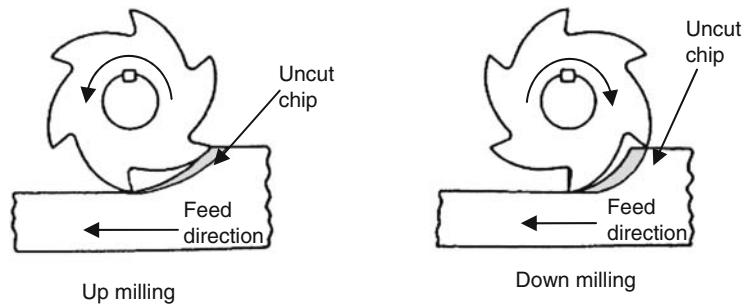


**Fig. 2.7** Illustration of up and down milling operations

and result in pushing the workpiece against the workholding surface. Cutting forces in milling are also not continuous. In up milling, the forces gradually increase from zero at beginning of tool engagement to a maximum when the cutting edge is about to leave the workpiece. Forces drop to zero again when the cutting edge leaves the workpiece.

Figure 2.8 shows a schematic of the cutting geometry for one cutting edge in up milling. The tool path is trochoidal and is generated from the combination of rotational (spindle) and translational (feed) motions. The exact geometry and kinematics of up and down milling have been thoroughly investigated by Martellotti [4, 5] and



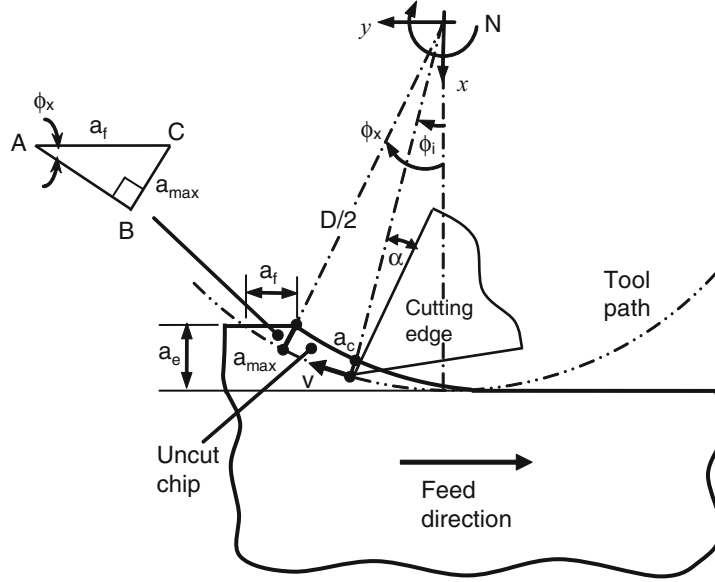


**Fig. 2.8** Cutting geometry in end milling, peripheral milling and edge trimming

Foenigsberger and Sabberwal [6] among others. The basic expressions describing this motion are given here. The cutting speed is given as a function of the spindle speed,  $N$ , and tool diameter,  $D$ , by the relationship

$$v = \pi DN. \quad (2.12)$$

The feed speed,  $v_f$ , and the feed per revolution,  $f$ , are related by

$$f = \frac{v_f}{N}. \quad (2.13)$$

The feed per tooth,  $a_f$ , which defines the translation of the workpiece between the engagement of successive cutting edges, is expressed as a function of the feed speed,  $v_f$ , the spindle speed,  $N$ , and the number of cutting edges on the cutterhead,  $T$

$$a_f = \frac{v_f}{TN}. \quad (2.14)$$

The length of the cutting edge engagement in the workpiece is given by the expression:

$$L_c = \frac{D}{2} \cos^{-1} \left( 1 - \frac{2a_e}{D} \right) \pm \frac{a_f T}{\pi D} (Da_e - a_e^2)^{1/2}, \quad (2.15)$$

where the plus sign is used for up milling and the negative sign is used for down milling. The average thickness of the undeformed chip is given by

$$a_{avg} = \frac{a_f a_e}{L_c}. \quad (2.16)$$

From these equations it is observed that the tool path is longer in up milling than in down milling. The uncut chip areas are the same for up milling and down milling, but the average chip thickness in down milling is greater. For a given depth of cut,  $a_e$ , the maximum uncut chip thickness for up milling is smaller than that for down milling. This explains the higher requirement of cutting power and the higher cutting forces associated with down milling.

For small feed speeds as compared to the spindle speed, the torchoidal path can be approximated by a circular arc and the uncut chip geometry for up and down milling becomes approximately the same. This happens to be the case for most machining applications of FRPs. The total engagement angle,  $\phi_x$ , is given as a function of the tool diameter and the radial depth of cut,  $a_e$

$$\cos\phi_x = 1 - \frac{2a_e}{D}. \quad (2.17)$$

The instantaneous uncut chip thickness,  $a_c$ , measured normal to the cutting path varies continuously with engagement angle,  $\phi_i$ , and is maximum at the exit angle  $\phi_x$ . A lead angle may be given to the cutting edge, similar to what is shown in Fig. 2.2, and results in thinning the uncut chip. The lead angle is  $90^\circ$  for peripheral and end milling. The maximum uncut chip thickness,  $a_{\max}$ , is calculated from the triangle ABC as

$$a_{\max} = a_f \sin\kappa \sin\phi_x. \quad (2.18)$$

For small depths of cut as compared to tool diameter, the maximum chip thickness can also be approximated by

$$a_{\max} = 2a_f \sqrt{\frac{a_e}{D}}. \quad (2.19)$$

The instantaneous uncut chip thickness,  $a_c$ , at engagement angle  $\phi_i$ , and the average chip thickness,  $a_{\text{avg}}$ , are given by:

$$a_c = a_f \sin\kappa \sin\phi_i \quad (2.20)$$

and

$$a_{\text{avg}} = a_f \sqrt{\frac{a_e}{D}}, \quad (2.21)$$

respectively. The length of chip being cut is approximated by

$$L_c = 0.5D \cos^{-1} \left( 1 - \frac{2a_e}{D} \right) \approx \sqrt{a_e D}. \quad (2.22)$$

The material removal rate,  $Z_w$ , in end milling is given by the products of the radial depth of cut,  $a_e$  axial depth of cut,  $a_p$ , and feed speed. In edge trimming and profiling,  $a_p$  represents the thickness of the workpiece

$$Z_w = a_e a_p v_f. \quad (2.23)$$

The time required for milling a length,  $L_w$ , is the time taken by the tool to traverse the length of the workpiece and any additional distance required to completely clear the tool off the workpiece. The machining time is given by:

$$t_m = \frac{L_w + L_e}{v_f}, \quad (2.24)$$

where  $L_e$  is the distance required to clear the workpiece by the tool and is given by

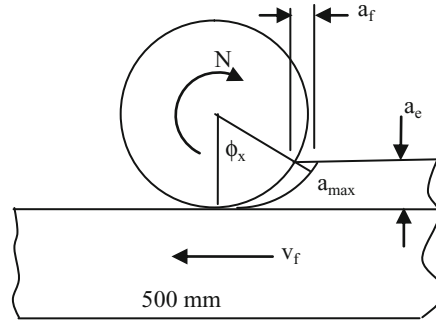
$$L_e = \sqrt{a_e(D - a_e)}. \quad (2.25)$$

*Example 2.1.* An edge trimming operation of particleboard uses a 19.0 mm cutterhead with one major cutting edge in a down-milling configuration. The spindle speed is 5,000 rpm and the feed rate is 1.27 m/min. The radial depth of cut is 1 mm, the length of workpiece is 500 mm and its thickness is 19 mm. The specific cutting power for particleboard is  $65 \text{ N/mm}^2$ . Determine:

- Total engagement angle
- Maximum chip thickness
- Material removal rate
- Time to finish one edge
- Power required for machining

*Solution*

The figure below shows the cutting geometry.



- Total engagement angle is given by

$$\phi_x = \cos^{-1} \left( 1 - \frac{2a_e}{D} \right) = \cos^{-1} \left( 1 - \frac{2(1)}{19} \right) = \cos^{-1} 0.895, \quad \phi_x = 26.5^\circ.$$

- Maximum chip thickness is given by

$$a_{\max} = \frac{v_f \sin \phi_x}{NT} = \frac{1.27 \sin 26.5}{1(5,000)} = 1.134 \times 10^{-4} \text{ m} = 0.113 \text{ mm},$$

where  $T = 1$  is the number of cutting edges on the cutterhead.

(c) Material removal rate is given by

$$Z_w = a_e a_p v_f = (1)(19)(1.27 \times 10^3) = 24,130 \text{ mm}^3/\text{min} = 402.2 \text{ mm}^3/\text{s}$$

(d) Time to trim one edge  $t_m = (L_w + L_e)/v_f$ , where  $L_e = \sqrt{a_e (D - a_e)}$

$$L_e = \sqrt{1(19 - 1)} = 4.24 \text{ mm},$$

$$t_m = (500 + 4.24)/1.27 \times 10^3 = 0.397 \text{ min} = 23.8 \text{ s}.$$

(e) Power required for machining

$$P_m = u_s Z_w = 65(402.2) = 26,141 \text{ Nmm/s} = 26.14 \text{ W}.$$

This is an average power that does not reflect the actual variation in chip thickness and hence, the instantaneous power consumption. The chip thickness varies with  $\phi_i$  according to the relationship

$$a_c = \frac{v_f \sin \phi_i}{NT} = \frac{1,270 \sin \phi_i}{1(5,000)} = 0.254 \sin \phi_i \text{ (mm)}.$$

The instantaneous chip area is

$$A_c = a_c a_p = 19(0.254 \sin \phi_i) = 4.826 \sin \phi_i \text{ (mm}^2\text{)}.$$

The instantaneous tangential cutting force is

$$F_{ti} = u_s A_{ci} = 65(4.826 \sin \phi_i) = 313.69 \sin \phi_i \text{ (N)}.$$

The instantaneous machining power is  $P_{mi} = F_{ti} v$ , where

$$v = \pi D N = (3.14)(19)(5,000) = 298,451.3 \text{ mm/min} = 4,974.2 \text{ mm/s}.$$

$$\text{Then } P_{mi} = 313.69 \sin \phi_i (4,974.2) = 1,560,356 \sin \phi_i \text{ (N mm/s)} = 1,560 \sin \phi_i \text{ (W)}.$$

The variation of power with  $\phi_i$  is given as:

$$\phi_i = 26.5^\circ, P_{mi} = 696 \text{ W (at entry)}$$

$$\phi_i = 13^\circ, P_{mi} = 351 \text{ W (halfway in the cut)}$$

$$\phi_i = 0, P_{mi} = 0 \text{ (at exit)}$$

## 2.5 Drilling

Drilling is the most common material removal operation in metals and composites machining. It is used for making holes required for assembly. Drilling is done on conventional upright drilling machines, milling machines, and various specialized machines. In drilling on a vertical drill press, the spindle provides the primary rotational motion to the drill bit and the feed into the workpiece is provided through the

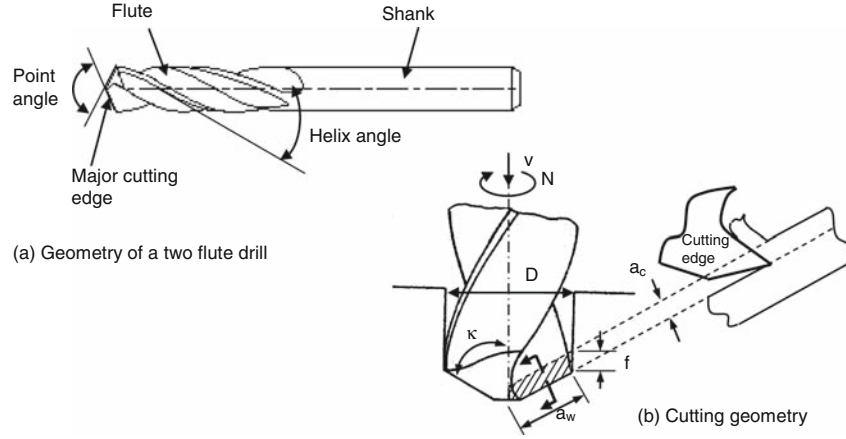


**Fig. 2.9** Cutting geometry in drilling

spindle axis. The most common drill bit is a two flute twist drill depicted in Fig. 2.9. A two flute twist drill has two major cutting edges forming the drill point angle. Each one of the major cutting edge acts like a single point cutting tool as shown in Fig. 2.9b. The lead angle for the cutting edge is half of the drill point angle. The flute provides a way for the chip to clear the cutting zone and for coolant to be supplied to the cutting tip.

For a drill of diameter  $D$ , which is being rotated by  $N$  revolutions per minute, the cutting speed is given by (2.12). The drill bit is feed into the workpiece with a feed per revolution,  $f$ . The feed speed,  $v_f$ , is related to the feed per revolution by

$$v_f = fN. \quad (2.26)$$

The feed per tooth is related to the feed per revolution and the number of flutes,  $T$ , by

$$a_f = \frac{f}{T}. \quad (2.27)$$

The width of the chip is related to the tool diameter and half the drill point angle,  $\kappa$  (also known as the lead angle) by

$$a_w = \frac{D}{2 \sin \kappa}. \quad (2.28)$$

The uncut chip thickness is given by

$$a_c = a_f \sin \kappa = \frac{f}{T} \sin \kappa. \quad (2.29)$$

The material removal rate,  $Z_w$ , is given by

$$Z_w = v_f \left( \frac{\pi D^2}{4} \right) = \frac{\pi f D^2 N}{4}. \quad (2.30)$$

The time required to drill a through hole in a workpiece of thickness,  $L_h$ , is calculated as the time required for the drill point to traverse the thickness and clear the drill cone. An additional distance,  $L_e$ , is required to clear the drill cone, which is given by

$$L_e = \frac{D}{2 \tan \kappa}. \quad (2.31)$$

The time to drill through the workpiece is given by

$$t_m = \frac{L_h + L_e}{v_f}. \quad (2.32)$$

*Example 2.2.* A two-flute twist drill is used to drill a hole in a particleboard that is 19 mm thick. The drill diameter is 5 mm, the drill point angle is  $90^\circ$ , and the spindle speed is 500 rpm and the feed rate is 0.5 mm/s. The specific cutting energy for particleboard is  $65 \text{ N/mm}^2$ . Determine:

- (a) The cutting speed
- (b) Maximum chip thickness
- (c) Material removal rate
- (d) The time required for drilling one hole
- (e) The power required for drilling

*Solution*

(a)  $v = \pi D N = (3.14)(5/1,000)(500) = 7.85 \text{ m/min}$ .

(b)  $f = \frac{v_f}{N} = \frac{0.5}{(500/60)} = 0.06 \text{ mm/rev}$ ,

$$a_c = a_f \sin \kappa = \frac{f}{T} \sin \kappa = (0.06/2) \sin 45^\circ = 0.0212 \text{ mm}.$$

(c)  $Z_w = v_f \left( \frac{\pi D^2}{4} \right) = \frac{\pi f D^2 N}{4} = \frac{(0.5)(3.14)(5^2)}{4} = 9.82 \text{ mm}^3/\text{s}$ .

(d)  $L_e = \frac{D}{2 \tan \kappa} = \frac{5}{2 \tan 45} = 2.5 \text{ mm}$ ,

$$t_m = \frac{19 + 2.5}{0.5} = 43 \text{ s}.$$

(e)  $P_m = u_s Z_w = 65(9.82) = 638.6 \text{ N mm/s} = 0.6386 \text{ W}$ .

Again, it is noted here that this power is not indicative of the cutting power, but rather the feed power. To determine the cutting power, follow the steps used in the milling example. Determine uncut chip thickness, estimate cutting forces, and determine torque and power from cutting forces

$$A_c = a_c a_w = \frac{f}{T} \sin \kappa \frac{D}{2 \sin \kappa} = \frac{f D}{2 T} = \frac{(0.06)(5)}{2(2)} = 0.075 \text{ mm}^2.$$

The tangential cutting force is estimated as

$$F_t = A_c u_s = 65(0.075) = 4.875 \text{ N}.$$

The torque required to overcome this force is calculated as

$$M = F_t D / 2 = 4.875(0.0025) = 0.0122 \text{ Nm.}$$

Finally, the machining power is calculated as

$$P_m = M(2\pi N/60) = 0.0122(2)(3.14)(500)/2 = 19.154 \text{ W.}$$

## 2.6 Abrasive Cutting

Abrasive wheels are commonly used in finishing operations of metals and ceramics where the resulting surface finish is the criterion. Abrasive wheels and cutters are also used in machining FRPs because they provide less mechanical damage and better surface finish than traditional cutting tool geometries. Examples of diamond abrasive cutting tools are shown in Fig. 2.10. In these tools, many diamond particles are brazed or bonded to the tool shank or body and act as multiple cutting points. Abrasive cutters are mainly classified by the abrasive particle size and the method by which the particles are bonded to the tool body. The size of abrasive particles is identified by a grit number, which is a function of sieve size. The smaller the sieve size, the larger the grit number.

Abrasive cutting is characterized mainly by negative rake angles, by small depths of cut, by wide edge angles, and by a limited grain protrusion as shown in Fig. 2.11. Each one of these diamond particles acts as a single point cutting tool and is responsible for removing a tiny chip ( $2\text{--}50\mu\text{m}$ ) as illustrated in this figure. Because each abrasive particle only removes a tiny chip at a time, many abrasive particles are needed to produce significant material removal rates. In addition, the power required for grinding is far higher than that for other machining operations because the specific cutting energy increases rapidly with a decrease in chip size.

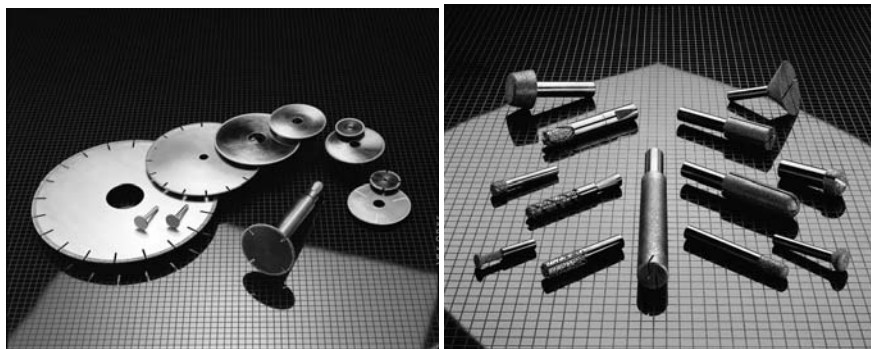


**Fig. 2.10** Diamond abrasive cutting wheels (*left*) and routers (*right*). Courtesy of Abrasive Technology, USA

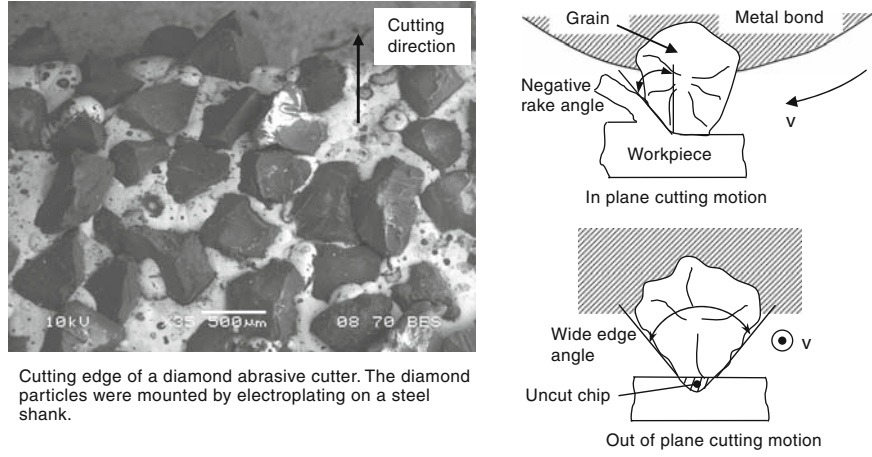


**Fig. 2.11** Multiple point cutting with negative rake in an abrasive cutter

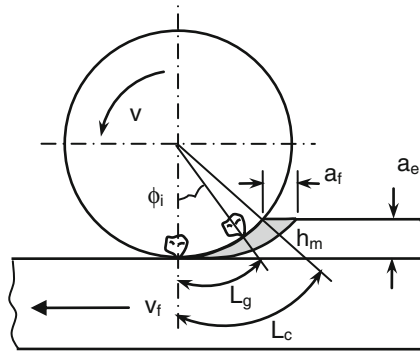


**Fig. 2.12** Material removal with abrasive cutter

Trimming with abrasive cutters is similar to trimming with an end mill and kinematic analysis of the tool path is similar. Detailed analysis of grinding and abrasive cutting is given in [3]. The cutter removes material in the form of a “comma”-shaped chip. In a real situation, this chip consists of many tiny “comma”-shaped chips, each of which is removed by an abrasive particle. For simplicity, an idealized distribution of the particles around the cutter periphery may be assumed where the particles are equally spaced by a distance  $L_g$  as shown in Fig. 2.12. The angular position,  $\phi_i$ , of grain  $G_i$  may be determined by (2.17). The cutting velocity of a cutting point is determined by (2.12). The feed per cutting point is equal to the product of the feed speed  $v_f$  and the time elapsed between successive cutting points,  $L_g/v$

$$a_f = \frac{L_g v_f}{v}. \quad (2.33)$$



The maximum uncut chip thickness taken by a cutting point is indicated by  $h_m$  and is determined from the expression:

$$h_m = 2a_f \left( \frac{a_e}{D} \right)^{1/2} \left( 1 - \frac{a_e}{D} \right)^{1/2} - \frac{a_f^2}{D} \quad (2.34)$$

and for small depths of cut as compared to tool diameter ( $a_e \ll D$ ),

$$h_m = 2a_f \left( \frac{a_e}{D} \right)^{1/2} - \frac{a_f^2}{D}. \quad (2.35)$$

Or substituting  $a_f$  from (2.33),

$$h_m = 2L_g \left( \frac{v_f}{v} \right) \left( \frac{a_e}{D} \right)^{1/2} - \frac{L_g^2}{D} \left( \frac{v_f}{v} \right)^2. \quad (2.35a)$$

The magnitude of  $h_m$  is typically an order of magnitude smaller than the depth of cut  $a_e$  and is much less than  $L_c$ . In this case the shape of the undeformed chip is nearly triangular. In order to calculate the undeformed chip thickness an estimate of the grain spacing,  $L_g$  is needed. A number of methods have been devised to measure wheel topography and obtain information on grain density  $C$ . The grain spacing is related the grain density and maximum chip thickness by

$$L_g = \frac{2}{Crh_m}, \quad (2.35b)$$

where  $r$  is the ratio of effective undeformed chip width to the average chip thickness,  $h_a$ . For  $h_m \ll L_c$  the average chip thickness is approximately half of the maximum chip thickness,  $h_a \cong 0.5h_m$ .

The contact length between the wheel and the workpiece,  $L_c$  can be determined using (2.15) or (2.22) by assuming the contact length to be a circular arc. This relationship can be adjusted to account for the feed motion, resulting into what is known as the kinematic contact length,  $L_k$ ,

$$L_k = L_c \left( 1 \pm \frac{1}{q} \right) + \frac{a_f}{2}, \quad (2.36)$$

where  $q = v/v_f$  and positive is used for up grinding and negative is used for down grinding. For most grinding applications  $v \gg v_f$  and the contribution of  $a_f$  is very small, in which case

$$L_k \approx L_c = \sqrt{a_e D}. \quad (2.37)$$

The material removal rate in abrasive cutting may be determined from the product of feed speed and the cross section of the chip normal to the feed speed,

$$Z_w = a_e \cdot a_p \cdot v_f. \quad (2.38)$$

Here,  $a_p$  denotes the width of the workpiece in edge trimming and the width of the cutter in peripheral grinding. The material removal rate can also be represented by a band of material of a uniform thickness  $h_q$  and width  $a_p$  that is being removed at the cutting speed  $v$ ,

$$Z_w = h_q \cdot a_p \cdot v. \quad (2.39)$$

The uniform thickness  $h_q$  is referred to as the equivalent chip thickness and is given by

$$h_q = a_e \frac{v_f}{v}. \quad (2.40)$$

The cutting time relationship for grinding is similar to that given for peripheral milling (2.24),

$$t_m = \frac{l_w + l_e}{v_f}. \quad (2.24)$$

In slot cutting with an abrasive wheel, the wheel makes a through-thickness slot in the workpiece which is fed relative to the wheel with a feed speed  $v_f$  as shown in Fig. 2.13. Many abrasive particles are engaged in the cut at one specific time, and the number of these particles or their distribution in the cutting region is difficult to determine. Therefore, it is not easy to determine the size of the chip removed by each abrasive particle. Instead, bulk quantities are determined. The material removal rate is determined by (2.38) where  $a_e$  is the workpiece thickness and  $a_p$  is the width of cut, which in this case is the width of the cutting wheel. The machining time is determined by (2.24) where  $l_e = 2\sqrt{a_e(D - a_e)}$  for  $z > 0$ . Because the wheel fully penetrates the workpiece, there are two engagement angles involved, one at entry and one at exit. At entry the engagement angle is determined by

$$\cos \phi_e = \frac{2z}{D}. \quad (2.41)$$

And at exit it is determined by:

$$\cos \phi_x = \frac{2(z + a_e)}{D}, \quad (2.42)$$

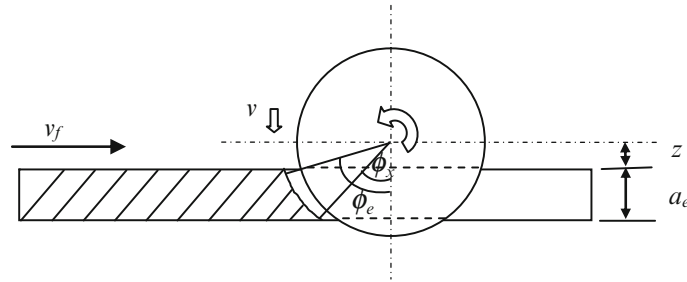


**Fig. 2.13** Cutting geometry for abrasive wheel slot cutting

where  $z$  is the distance between the wheel center and the top surface of the workpiece.

## 2.7 Surface Finish

In a machining process, a specific surface geometry is produced as a result of the prescribed machine tool kinematics. This surface geometry is called an ideal or theoretical surface geometry, which follows a repeated pattern. In real life, however, the actual machined surface deviates from the ideal surface because of the occurrence of tool wear, machine vibrations, material inhomogeneity, and other factors not related to machine tool kinematics. The actual machined surface may not have a regular geometry. These effects result in what is called natural surface finish. Figure 2.14 shows the different definitions used to describe machined surface geometric characteristics. The surface profile is typically described by its lay, waviness, and roughness.

Lay is the macroscopic contour of the surface and describes the direction of the predominant surface pattern. The term lay is mostly used to describe flat surfaces and shape is used for contoured surfaces. Errors in lay and shape result from misalignment of machine components and from distortions resulting from clamping forces. Waviness is the recurrent deviations from an ideal surface that are relatively of large magnitude ( $>0.1$  mm). These deviations result from deflections in the machine tool and cutting tool, from errors in the tool geometry and from machine vibrations. Roughness is the finely spaced irregularities or irregular deviations characterized by short wavelength as shown in Fig. 2.14. Roughness is affected by tool shape and feed (ideal surface finish) as well as by machining conditions (natural surface finish).

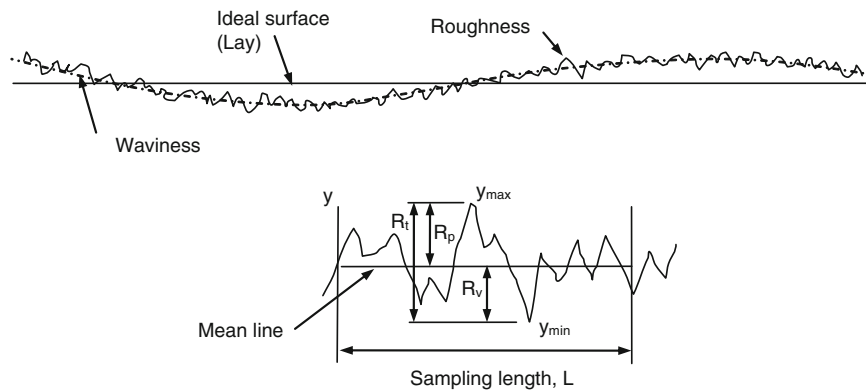


**Fig. 2.14** Schematic representation of a machined surface

Surface roughness is most often used to characterize machined surfaces. It is commonly quantified by statistical parameters such as the arithmetic mean value  $R_a$ , maximum peak to valley height  $R_t$ , maximum peak to mean height  $R_p$ , mean to valley height  $R_v$ , and ten point average height  $R_z$ . Machined surface profile is most commonly measured by a stylus surface profilometer. Modern profilometers trace the machined surface over a prescribed sampling distance and compute the statistical parameters for the user. A representative surface profile is shown in Fig. 2.14 for the purpose of illustrating the statistical parameters. For a sampling length,  $L$ , the surface variations are described as a function of distance  $x$ ,  $y = f(x)$ . The mean line of the profile for this segment is determined as

$$\bar{y} = \frac{1}{L} \int_0^L y dx \quad (2.43)$$

The maximum peak-to-valley height within the sampling length is determined by

$$R_t = y_{\max} - y_{\min}. \quad (2.44)$$

The maximum peak-to-mean height and valley-to-mean height are determined, respectively, by

$$R_p = y_{\max} - \bar{y} \quad (2.45)$$

and

$$R_v = \bar{y} - y_{\min}. \quad (2.46)$$

The average of the numerical deviations from the mean line of the surface within the sample length,  $R_a$  is determined by

$$R_a = \frac{1}{L} \int_0^L |y - \bar{y}| dx. \quad (2.47)$$

Finally, the ten-point average,  $R_z$  is determined as the difference between the five greatest peaks and the five lowest valleys within the sampling length

$$R_z = \frac{1}{5} \left( \sum_1^5 y_i^p - \sum_1^5 y_i^v \right). \quad (2.48)$$

The ideal roughness of machined surfaces depends primarily on cutting edge geometry and feed rate. Figure 2.15 shows the ideal surfaces generated when turning with a sharp tool and a round cornered tool. For a sharp cornered tool, the surface roughness can be determined geometrically as a function of the feed rate,  $f$ , and the major and minor cutting edge angles,  $\kappa$  and  $\kappa'$ , respectively [1]:

$$R_t = \frac{f}{\cot \kappa + \cot \kappa'}, \quad (2.49)$$

$$R_a = \frac{f}{4(\cot \kappa + \cot \kappa')}. \quad (2.50)$$

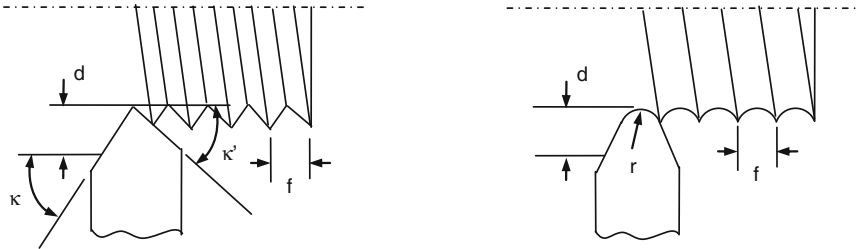


**Fig. 2.15** Ideal surface roughness obtained in turning with a sharp tool and rounded tool

**Table 2.1** Ranges of ideal surface roughness for selected material removal operations

Process	Roughness $R_a$ ( $\mu\text{m}$ )
Turning	3–12
Planing	3–12
Drilling	3–25
Milling	1–10
Grinding	0.25–3

For a round cornered tool, it can be shown that [1]:

$$R_t \cong \frac{f^2}{8r}, \quad (2.51)$$

$$R_a \cong \frac{f^2}{32r}, \quad (2.52)$$

where  $r$  is the tool corner radius.

Equation (2.51) can also be used to approximate the surface roughness for end milling (trimming). In this case,  $f$  becomes equal to  $a_f$  and  $r$  becomes the cutter radius,  $D/2$ . For abrasive cutting  $a_f = v_f L_g / v$ , where  $L_g$  is the spacing around the periphery between successive cutting points. Equations (2.51) and (2.52) become [3]:

$$R_t \cong \frac{1}{4} \left( \frac{v_f L_g}{v D^{1/2}} \right)^2, \quad (2.53)$$

$$R_a \cong \frac{1}{9\sqrt{3}} \left( \frac{v_f L_g}{v D^{1/2}} \right)^2. \quad (2.54)$$

As illustrative information, Table 2.1 gives typical roughness values for different processes corresponding to normal workshop practice.

**Example 2.3.** An edge trimming operation of particleboard uses a 19.0 mm cutter with one cutting edge in a down-milling configuration. The spindle speed is 5,000 rpm and the feed rate is 1.27 m/min. Determine the effect of the following on surface roughness  $R_t$  and  $R_a$ :

- Doubling the number of teeth
- Doubling feed rate

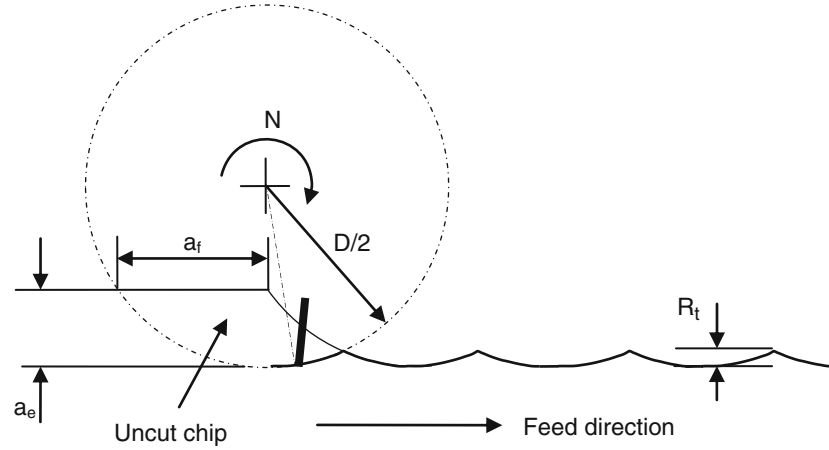


**Fig. 2.16** Cutting geometry for Example 2.3

**Table 2.2** Effect of cutting parameters on ideal surface roughness in edge trimming

Parameter	$a_f = \frac{v_f}{NT}$	$R_t$	$R_a$
$r = 9.5 \text{ mm}$ $v_f = 1.27 \text{ m/min}$ $N = 5,000 \text{ rpm}$ $T = 1$	0.254 mm	$0.85 \mu\text{m}$	$0.21 \mu\text{m}$
(a) $T = 2$ All other parameters remain unchanged	0.127 mm	$0.21 \mu\text{m}$ (75% decrease)	$0.05 \mu\text{m}$ (76% decrease)
(b) $v_f = 2.54 \text{ m/min}$ All other parameters remain unchanged	0.508 mm	$3.40 \mu\text{m}$ (300% increase)	$0.85 \mu\text{m}$ (300% increase)
(c) $r = 19.0 \text{ mm}$ All other parameters remain unchanged	0.254 mm	$0.42 \mu\text{m}$ (50% decrease)	$0.11 \mu\text{m}$ (50% decrease)
(d) $N = 10,000 \text{ rpm}$ All other parameters remain unchanged	0.127 mm	$0.21 \mu\text{m}$ (75% decrease)	$0.05 \mu\text{m}$ (75% decrease)

(c) Doubling cutter diameter.

(d) Doubling spindle speed

Geometry of the trimmed surface is shown in Fig. 2.16. The size of chip per tooth and the resulted uncut chip are exaggerated for clarity. As a first approximation it is assumed that the cutter completes one turn then intermittently advances a distance  $a_f$ , as opposed to a continuous path prescribed by a torchoid. This allows the surface profile to be approximated by (2.50) and (2.51) after replacing  $f$  with  $a_f$  and  $r$  with  $D/2$

$$R_t = \frac{a_f^2}{8(D/2)} \text{ and } R_a = \frac{a_f^2}{32(D/2)}. \quad (2.55)$$

The effect of (a), (b), (c), and (d) on surface roughness is shown in Table 2.2. It is apparent that significant reduction in  $R_a$  and  $R_t$  can be obtained by doubling number of teeth, doubling spindle speed or reducing feed rate in half.

## 2.8 Summary

Machining of composites is necessary for finishing parts to the required tolerances and for preparing components for subsequent assembly. Conventional machining processes such as turning, milling, drilling, abrasive cutting, and grinding are used to generate complex features by removing material in the form of tiny chips. The machining process takes place as a result of engaging a rigid cutting tool into the workpiece and prescribing the necessary relative motions between the tool–work pair that will result in material removal and generating new surfaces. The size and shape of the chip removed, material removal rate and resulting ideal surface finish are closely related to the kinematic relationships between the cutting tool and the workpiece.

Turning utilizes a single point cutting tool that is steadily feed against a rotating workpiece in order to generate cylindrical surfaces. The key process parameters that affect the turning process outcome are tool geometry, feed rate, depth of cut, and rotational speed. The cross-sectional area of the chip removed is proportional to the product of feed rate and depth of cut, while material removal rate is a function of the speed by which this cross section is swept. The ideal roughness of the machined surface is proportional to the square of feed rate and is inversely proportional to the cutting edge nose radius. Drilling is another process that produces circular surfaces (holes). The difference between drilling and turning, however, is that in drilling the cutting edge is rotated and advanced along its axis of rotation, as opposed to a nonrotating cutting edge in turning. Nevertheless, most of the kinematic relations in drilling are similar to those in turning.

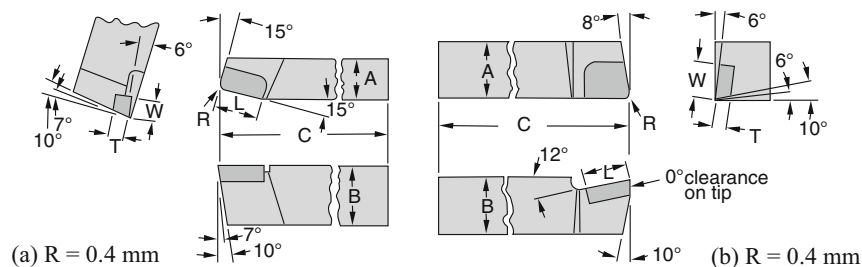
In a milling process, the cutting tool which often has multiple cutting edges rotates around its axis while a translation motion (feed motion) is introduced relative to the workpiece. Milling is capable of producing complex contoured surfaces. Depending on the relationship between the feed motion and the rotational motion, either up milling or down milling is produced. Up (conventional) milling is produced when the rotational speed and feed speed are in opposite directions whereas down (climb) milling is produced when the two motions are in the same direction. In both cases, the thickness of chip removed is not constant and continuously changes from cutting edge entry to exit. The chip thickness is a function of the cutting edge position along the cutting circle and the feed speed. The material removal rate in milling is proportional to the width of cut, depth of cut, and feed speed. Similar to turning, the ideal surface roughness is proportional to the feed speed and is inversely proportional to the tool radius. Abrasive machining is similar to milling in a way that material removal is caused by the engagement of tiny cutting edges of the abrasive

grit. However, the material removal rate is much smaller and surface roughness is much better than those in milling.

Even though most of the conventional machining practices are well established and have substantial supportive data bases for metal machining, their application to machining FRPs is relatively new and the necessary expertise is lacking. It is imperative that one recognizes the differences in machining FRPs as compared to metals. Unlike metals, FRPs are inhomogeneous materials that generally fail by brittle fracture. Thus the concept of continuous chip formation that is characteristic of metal machining does not exist in machining FRPs. The machining characteristics such as surface finish and cutting forces are strongly influenced by the reinforcement volume fraction, form, and orientation. The requirements of machining FRPs include a sharp cutting edge in order to shear effectively the fibers, low material removal rates, and lower temperatures than those encountered in metal machining.

## Review Questions and Problems

1. Define cutting speed, feed, chip thickness, chip width, uncut chip area, and material removal rate for turning, drilling, and milling.
2. What is the significance of material removal rate and specific cutting pressure in machining process selection and design?
3. Identify the tool signature: major (side) cutting edge, minor (end) cutting edge, cutting-edge inclination, corner (nose) radius, tool face, and major and minor flanks for the cutting tools shown below. Refer to Fig. 2.3 for terminology.



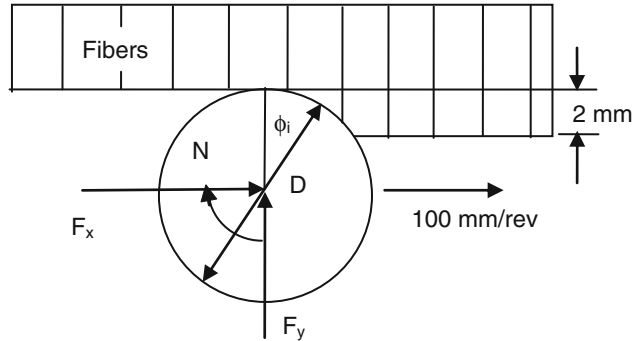
4. The rpm for a 1.00-in. diameter piece of stock that is being turned at a cutting speed of 400 sfpm is (show calculations):  
(a) 450 (b) 1,528 (c) 764 (d) 532
5. The feed speed for a two (2) toothed milling cutter that is being rotated at 500 rpm while cutting 0.002 in. per tooth is (show calculations):  
(a) 4.0 ipm (b) 2.0 ipm (c) 8.0 ipm (d) 0.02 ipm
6. It is required to turn down a 10.0-in. long rod from a 3.0-in. diameter to a 2.5-in. diameter using a depth of cut of 0.1-in., a feed speed of 0.05 ipr and a spindle speed of 900 rpm. The total cutting time required is (show calculations):  
(a) 13.30 s (b) 0.67 s (c) 40 s (d) 13.30 min



7. It is required to finish-turn the diameter of a glass-fiber-reinforced axle from 77.0 to 75.0 mm at a length of 50.0 mm on each end of the axle. The axle is 1,000.0 mm long. The axle is turned at 800 rpm, the feed is 0.1 mm/rev and the depth of cut is 1.0 mm. Determine the material removal rate, cutting power, and the cutting time required for finish-turning one axle. Use a specific cutting energy for glass FRPs of approximately 500 N/m<sup>2</sup>.



8. In a drilling operation using a twist drill, the rotational frequency of a drill is  $5 \text{ s}^{-1}$ , the feed 0.25 mm, the major cutting-edge angle  $60^\circ$ , and the drill diameter 12 mm. Assuming that the specific cutting energy of the work material is  $0.75 \text{ GJ/m}^3$ , calculate:
- The maximum material removal rate
  - The undeformed chip thickness
  - The drill torque, in Newton-meter
9. In a turning application of a glass/epoxy composite, an unsatisfactory surface roughness was produced. Which one of the following actions would you recommend in order to improve surface roughness? Justify your answer by reference to pertinent material in class notes.
- Increase cutting speed
  - Increase feed speed
  - Increase both cutting speed and feed speed
  - Decrease cutting speed
  - Decrease feed speed
  - Decrease both cutting speed and feed speed
  - Other action – explain
10. In a down end-milling operation, the thickness of the workpiece is 11 mm, its length is 200 mm, and the radial depth of cut is 1 mm. The cutter has four straight flutes and a diameter of 10 mm. The spindle speed is 2,000 rpm and the feed speed is 1,270 mm/min. Determine the following:
- The maximum undeformed chip thickness
  - The feed per tooth
  - The entry angle, exit angle, and total angle of engagement of the cutter
  - The maximum material removal rate
11. Consider a milling operation of unidirectional CFRP with a cutter diameter of 20 mm, and one cutting edge on the cutter. The cutter speed is 1,000 rpm, the feed speed is 100 mm/rev, and the depth of cut is 2 mm. The thickness of the workpiece is 4.0 mm. A schematic of the cutting configuration is shown below.



- (a) Determine the total engagement angle  $\phi_x$ .
- (b) Determine the instantaneous fiber orientation angle  $\theta_i$ , which is the angle between the fibers and the cutting velocity vector, as a function of the instantaneous engagement angle  $\phi_i$ . Evaluate the fiber orientation angle for an instant that is halfway between entry and exit of the cutting edge.

## References

1. Boothroyd, G., Knight, W., Fundamentals of Machining and Machine Tools, 2nd Edition, Marcel Dekker, New York, NY, 1989.
2. Stephenson, D., Agapiou, J., Dekker, M., Metal Cutting Theory and Practice, Marcel Dekker, New York, NY, 1997.
3. Stephen, M., Grinding Technology, Society of Manufacturing Engineers, Industrial Press, New York, NY, 1989.
4. Martellotti, M. E., An analysis of the milling process. Transactions of ASME 63, 677–700, 1941.
5. Martellotti, M. E., An analysis of the milling process, part-ii down milling. Transactions of ASME 67, 233–251, 1945.
6. Koenigsberger, F., Sabberwal, A.J.P., Chip section and cutting force during the milling operation. CIRP Annals 10, 197–203, 1961.



<http://www.springer.com/978-0-387-35539-9>

Machining of Polymer Composites

Ahmad, J.

2009, XII, 315 p., Hardcover

ISBN: 978-0-387-35539-9